aspects observed following 45 days' incubation of 4 blood specimens are reported.

The observations here described indicate that the corynebacteria-like forms taken under consideration in the course of the present research undergo, through a great variety of morphological appearances, a developmental cycle fairly referable to the one already described in the literature[14].

The present observations appear to be in accordance with the point of view of Pease[9,11,12] concerning the association of the infection with the erythrocytes, and also with previous data[15] related to the intraerythrocytic growth patterns of the cell wall deficient variants of other microbial forms.

1 G.G. Tedeschi, D. Amici and M. Paparelli, Nature *222*, 1285 (1969).
2 G.G. Tedeschi, D. Amici and M. Paparelli, Haematologia *4*, 27 (1970).
3 G.G. Tedeschi and D. Amici, It. J. Biochem. *24*, 102 (1975).
4 G.G. Tedeschi, D. Amici and I. Santarelli, Experientia *31*, 1088 (1975).
5 G.G. Tedeschi, D. Amici and I. Santarelli, Experientia *32*, 925 (1976).
6 G.G. Tedeschi, D. Amici, I. Santarelli, M. Paparelli and C. Vitali, in: Microbial Ultrastructure, Technical Series No. *10*, p. 325. Academic Press, London 1976.
7 G.G. Tedeschi and I. Santarelli, in: Spheroplasts, Protoplasts and L-forms of Bacteria, vol. 64, p. 341. Ed. INSERM, Paris 1977.
8 G.G. Tedeschi and D. Amici, Annali Sclavo *14*, 430 (1972).
9 P. Pease, Ann. rheum. Dis. *33*, 67 (1974).
10 K.A. Bisset, Ann. rheum. Dis. *36*, 96 (1977).
11 P. Pease, Ann. rheum. Dis. *28*, 270 (1969).
12 P. Pease, Ann. rheum. Dis. *29*, 439 (1970).
13 Bergey's Manual of Determinative Bacteriology, 8th ed. The Williams & Wilkins Co., Baltimore 1974.
14 K.A. Bisset, in: The Cytology and Life-History of Bacteria, 3rd ed., p. 98. E. & S. Livingstone, Edinburgh and London 1970.
15 L.H. Mattman, in: Cell Wall Deficient Forms, p. 188. CRC Press, Inc., Cleveland, Ohio 1974.

The ultrastructure of the spiral notosetae of *Nicomache maculata* Arwidsson (Polychaeta, Maldanidae)

B. Kennedy and H. Kryvi

Institute of Anatomy, University of Bergen, Årstadveien 19, N-5000 Bergen (Norway), 28 September 1977

Summary. Scanning- and transmission electron microscopy show that the long, thin notosetae of *Nicomache maculata* are helical over much of their length, and that their finely feathered appearance is produced by a series of minutely spiny scales. The internal structure varies considerably from one end of the seta to the other. While a helical shape could result from a rotating or asymmetrical secretion-rate gradient across the chaetoblast, we raise the possibility that the spiral represents a warp in the seta following deposition of the setal material.

A tremendous variety of setae are produced by polychaetes. Among the more spectacular of these are the extremely long and thin spiral notosetae on the posterior segments of some Maldanidae. The setae are visible in a good dissection microscope, and they appear in some of the older figures of *Nicomache* species[1]. They are not always figured as having a helical shape, however, and the details of their surface features, beyond the resolving capacity of even the best light microscopes, have been variously interpreted. Here we present some results of an examination using scanning electron microscopy (SEM) and transmission electron microscopy (TEM) of these remarkable setae in *Nicomache maculata*, with some measurements and comments on their structural properties.

We collected the specimens from the shore near the Dove Marine Laboratory[2], Cullercoats (England) and processed them for SEM and TEM as described elsewhere[3,4].

The long, thin setae of species of *Nicomache* have been described as wavy or sinuous[5,6]. Viewed from different angles in the dissection microscope, these setae in *Nicomache maculata* appear helical rather than wavy in either living or fixed material, and our SEMs (figure, A and B) show they are spiral over much of their length. In our larger specimens, whose perianal funnel is about 2 mm in diameter, the longest of the spiral setae may be combed straight with a forceps to a length of more than 3 mm.

The feathered[5,7] or pinnate[6] appearance of these setae in the light microscope is produced by an arrangement of minute spines (figure, C–G). At their fullest development, these spines are grouped to form a series of partially overlapping, distally pointed, featherlike scales, each wrapped around the setal axis. Each scale is grossly asymmetrical, such that the shorter edge of each scale (figure, E, s) meets the longer edge of a more distal scale (figure, E, l) at a point only part way around the seta (figures E, p; J, f).

Near its proximal end (not figured), a fully-grown spiral seta has a structure characteristic of setal shafts from other polychaetes[8–11]. The shaft is a cylindrical bundle of tubules of various diameters, from up to 0.8 µm near the axis to 0.3 µm or smaller at the periphery. The tubules are cylindrical, so that while they are closely packed, there are electron-translucent spaces among them. The electron opaque wall of each tubule encloses an electron-translucent lumen irregularly traversed by fine strands.

More distally, where the shaft emerges from the body wall (figure, H), the boundaries of most of the tubules are obscured by electron-opaque material, and the lumens are narrower than near the proximal end. The spatial arrangement of the centres of the tubules is like that more basally, however, and a few electron-translucent packing faults are visible. Still more distally (figure, I), nearly all the lumens are reduced to small points in section. Here, however, the boundaries of the tightly-packed tubules appear as electron-translucent polygonal outlines. Some of the outer polygons appear to be joined, and large numbers of very small ones gather just within the margin.

Over most of its length, the seta is decorated by spines, and throughout this region (figures, J and K) the tubules described from the shaft are either absent or obscured by other features. Small irregular or circular electron-translucent spaces appear, but they are not arranged as described above, nor can they be traced very far through serial sections. Each spine contains a tiny lumen (figures, K and L) which can be traced to the point where the spine merges with the setal axis.

The specific shape of a polychaete seta is produced by changes in the form of the apical surface of the chaetoblast upon which it is molded during basal appositional growth[12].

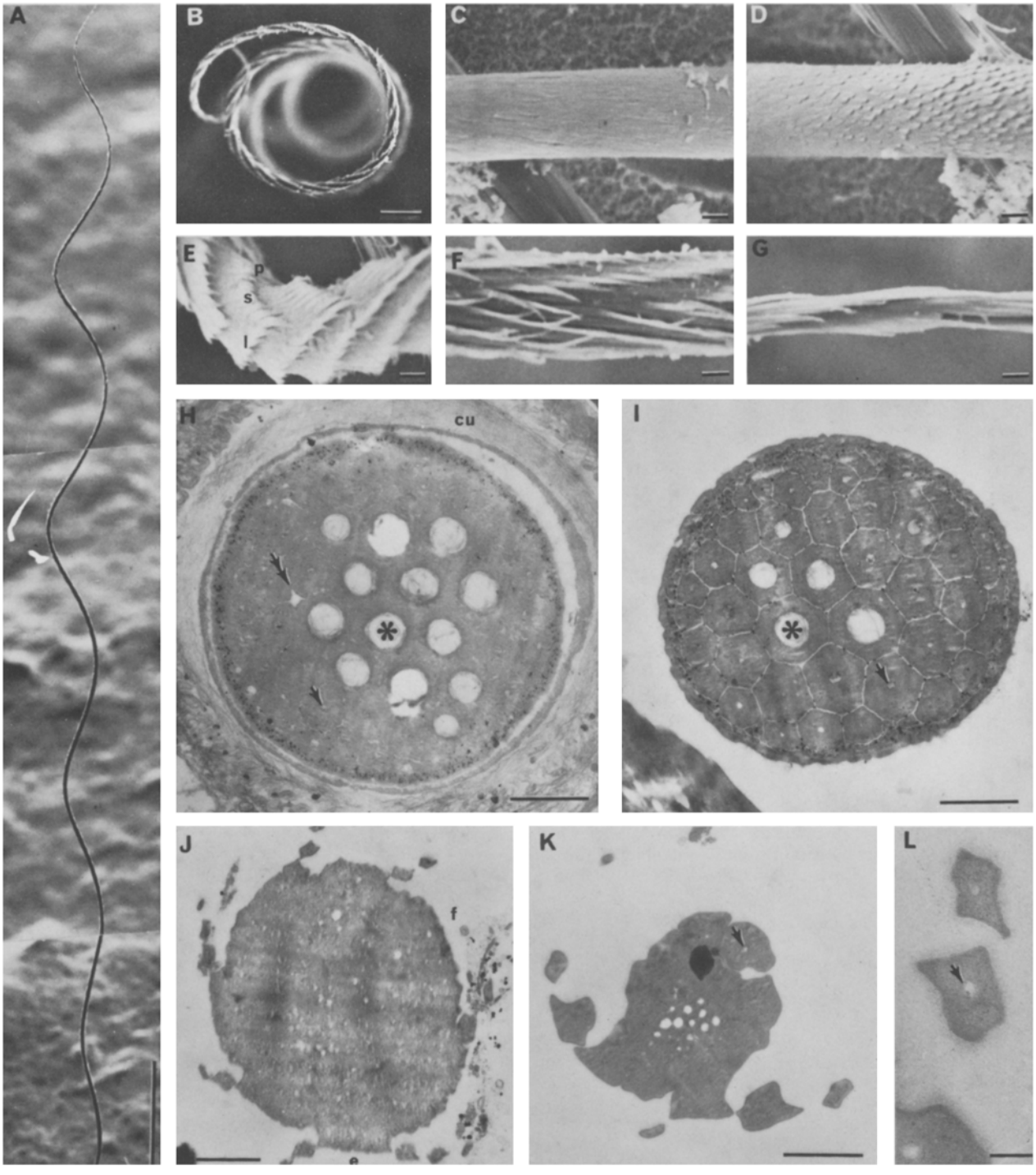

Scanning electron micrographs (A–G) and transmission electron micrographs of transverse sections (H–L) of spiral notosetae of *Nicomache maculata*. *A* Distal portion, standing erect and unsupported over the specimen stub. *B* Same seta as in figure A, but here viewed end-on. Focus is on the 1st turn of the helix below the tip. *C* Shaft near the point where it emerges from the body wall. *D* Shaft more distally, where the more basal spines emerge. *E* Still more distally, where the spines reach their greatest development. *F* As in figure E, but viewed from an opposite direction. *G* Very near the tip. *H* Shaft just basal to its emergence from the body wall. It is loosely invested by the cuticle of the setal follicle, cu. Circular electron-translucent spaces (e.g., *) are interpreted as tracks left during setal growth by microvilli on the chaetoblast; angular spaces (e.g., double arrow) as packing faults among the tubules of setal material (electron-opaque) molded on the microvilli. More peripheral lumens (e.g., arrow) are nearly filled with setal substance. *I* Shaft at about the level shown in figure C. Lumens of most of the tubules (e.g., arrow) are here filled; only a few spacious lumens are present (e.g., *). *J* Level where the spines have reached their fullest development, showing profiles of surfaces seen in figures E (e) and F (f). Only traces of the tubules seen in the shaft are visible here. *K* Level shown in figure G. *L* Enlargement of spine profiles from level shown in figure G. Scale lines on the figures indicate: *A*, 100 µm; *B*, 10 µm; *C–K*, 1 µm; *L*, 0.1 µm.

Circular lumens in the tubules of the setal shaft, as well as in its ornamentations, are interpreted as tracks of dynamic microvilli[4,8,13].

If the apical surface of the chaetoblast secretes material near one margin at a greater rate than near the opposite one, then a curved seta might result. A helical seta might result if such a gradient of secretion rate were appropriately asymmetrical, or if it rotated about the setal axis. The diameter of the seta in figures, A and B is about 4 µm, while each turn of the helix is about 250 µm long and about 50 µm across. This geometry would be expected from a gradient only 4% greater on one side than on the other.

On the other hand, the arrangement of scales imposes a structural heterogeneity across the seta at any point. A physical change in the setal material after deposit on the chaetoblast template, such as shrinkage, would perhaps be reflected in warping of the seta. Because the scales are asymmetrical and arranged in a series which itself takes a spiral course about the setal axis, such a warp would be expected to assume a helical form. We have no direct evidence that such a physical change occurs. The hypothesis might be tested by comparison of the arrangements of spines on the straight, or only slightly helical, long, thin setae of other maldanids.

1 I. Arwidsson, Proc. R. Irish Acad. *29*, 209 (1911).
2 We thank Dr P.J.W. Olive for calling our attention to the material.
3 B. Kennedy and H. Kryvi, manuscript submitted to Zool. Scripta.
4 B. Kennedy and H. Kryvi, manuscript in preparation.
5 G. Hartmann-Schröder, Tierwelt Deutschlands *58*, (1971).
6 P. Fauvel, Faune Fr. *16*, (1927).
7 J.H. Day, Polychaeta of Southern Africa. 2. Sedentaria (1967).
8 Y. Bouligand, Z. Zellforsch. *79*, 332 (1967).
9 J.D. George and E.C. Southward, J. mar. biol. Assoc. U. K. *53*, 403 (1973).
10 L. Orrhage, Acta zool., Stockh. *52*, 157 (1971).
11 H. Scherf, Zool. Jb. Anat. *87*, 386 (1970).
12 G. Bobin, Annls Inst. oceanogr., Monaco *22*, 1 (1944).
13 R.M. O'Clair and R.A. Cloney, Cell Tissue Res. *151*, 141 (1974).

Cell surface proteolytic activity of suspended embryonic cells isolated with and without proteolytic enzyme

L.L. Wiseman and W.R. Hammond

Department of Biology, The College of William and Mary, Williamsburg (Virginia 23185, USA), 5 September 1977

Summary. Although trypsin-disaggregated embryonic chick neural retina cells are incapable while EDTA-disaggregated cells are capable of immediate aggregation in culture, cells from both populations exhibit equally negligible levels of cell surface proteolytic activity as measured by substrate assay. The trypsin-induced lag does not appear, therefore, to depend upon adsorbed enzyme.

Embryonic chick cells isolated by proteolytic treatment are not immediately adhesive[1,2]. Suspensions of cells in rotation culture are capable of aggregation only after a variable period of time, depending upon cell type and enzyme preparation. On the other hand, cells isolated without enzymatic treatment (e.g. with EDTA) aggregate immediately without a lag. One possible explanation for the aggregation lag is that active enzyme is adsorbed to cell surfaces and interferes with subsequent cell-cell interactions. Trypsin can be adsorbed to various substrates[3] and cells treated with trypsin are reported to digest extracellular protein[4]. However, it has been demonstrated that although trypsin activity is eliminated by either soybean trypsin inhibitor or serum, neither treatment abolishes the aggregation lag of enzymatically isolated cells[1].

We wished to test directly for the presence of proteolytic activity on the surfaces of isolated cells. EDTA-isolated cells, capable of immediate aggregation, and trypsin-isolated cells, requiring time to become aggregation competent, were assayed for surface proteolytic activity. Neural retina cells were isolated from 7 day White Leghorn chick embryos by standard procedures used in our laboratory[5], using either 0.1% crude trypsin (1:250 Difco) or 1.0% EDTA, each prepared in calcium and magnesium-free Hanks' balanced salt solution. Isolated cells were washed in 10% horse serum and in Hanks' solution.

Azocoll (Calbiochem), an insoluble, powdered cowhide containing assorted peptide linkages, to which a red dye is attached, served as substrate. 25 mg Azocoll was suspended in 5 ml phosphate buffered saline (pH 7.0) in test tubes containing 1×10^6 cells per ml. The mixture was incubated for 15 min at 37 °C in either a stationary water bath or on a test tube rotator at 60 rpm. After incubation the tubes were centrifuged and the supernatant, free of cells and Azocoll particles, was examined spectrophotometrically at 520 nm for the presence of released dye. Azocoll plus 0.1% crude trypsin, with and without soybean trypsin inhibitor (Sigma), served as controls.

The table gives the results. Crude trypsin alone, as expected, easily digested the Azocoll substrate as indicated by the release of red dye. The supernatant was deep red and absorbance at 520 nm was high. Soybean trypsin inhibitor reduced proteolytic activity in the assay system.

Cells isolated by either crude trypsin or by EDTA showed

Optical density readings at 520 nm for Azocoll assay

Constituents added to Azocoll	Stationary water bath, 37 °C	Test tube rotator 37 °C, 60 rpm
0.1% Crude trypsin	2+	2+
0.1% Crude trypsin and 0.05% soybean trypsin inhibitor	1.4	1.8
0.1% Crude trypsin and 0.2% soybean trypsin inhibitor	-	0.48
Cells isolated with 0.1% crude trypsin	0.01	0.02
Cells isolated with 1.0% EDTA	0.01	0.01